Kinematic Analysis and Distinct Element Modelling of a polyphase Rock Fall

Reinhard Gerstner, Christine Fey, Klaus Voit, Erik Kuschel
Institute of Applied Geology, University of Natural Resources and Life Sciences, Vienna (BOKU), Austria

Gerald Valentin
Landesgeologischer Dienst, Land Salzburg, Austria

Christian Zangerl
Institute of Applied Geology, University of Natural Resources and Life Sciences, Vienna (BOKU), Austria

ABSTRACT: Rock falls are one of the most hazardous mountain processes and can show variable failure mechanisms. Therefore, a kinematic analysis is commonly performed to assess which failure mechanisms are favoured by the structural inventory of a rock mass. However, often multiple failure mechanisms are thereby considered possible. In our paper, we emphasize this ambiguity and investigate factors controlling the actual rock fall failure mechanism.

For this purpose, we have selected a case study in southern Salzburg (Austria), where three rock falls occurred from a highly schistose, metamorphic rock mass in the year of 2019. In our study, we characterized the structural inventory of the rock mass hosting the rock falls and identified possible failure mechanisms by a kinematic analysis. Through distinct element modelling, we show that depending on the persistence of pre-existing structures, the reproduced failure mechanism alternates between the kinematically proposed mechanisms, i.e. block toppling and sliding.

Keywords: rock fall, initial failure mechanism, kinematic analysis, structural control, distinct element modelling.

1 INTRODUCTION

Rock falls (Hungr et al. 2014) are widespread hazard processes in mountainous regions, e.g. Crosta et al. (2015), and can have a devastating effect on human lives and infrastructure. Therefore, it is of great scientific and public interest to improve our knowledge concerning the initial rock slope failure and subsequent movement mechanisms underlying rock fall processes.

A rock slope can fail by different kinematic mechanisms, such as sliding, toppling, or falling (e.g. Zangerl et al. 2008). These mechanisms can be divided into sub-mechanisms with specific characteristics and structural predisposition conditions. For rock toppling, these sub-mechanisms are flexural, block, or block-flexure toppling (Goodman & Bray 1976), and for rock sliding, for example, planar or wedge sliding (Hungr et al. 2014).

However, during a rock fall process, the deformation mechanism may change. Thus, it is also essential to distinguish between the initial failure mechanism on the one hand and possible running-out mechanisms on the other (Poisel & Preh 2004).

For a comprehensive hazard assessment and the selection of appropriate monitoring techniques as well as mitigation measures, identification of these potential initial failure mechanisms is crucial. Therefore, a kinematic analysis is commonly performed for natural and engineered slopes (Wyllie & Mah 2004), taking the structural inventory relative to the orientation of the investigated slope into account. This analysis allows for assessing which failure mechanisms are kinematically possible. However, several different failure mechanisms are often considered probable thereby.

The objective of this contribution is to emphasize this ambiguity and to investigate which factors control the actual failure mechanism, which is often more complex in nature, than suggested by a kinematic analysis. For this purpose, we have selected a case study in southern Salzburg.

2 THE HÜTTSCHLAG ROCK FALL

In the municipality of Karteis/Hüttschlag, located in the Großarl Valley in southern Salzburg, Austria (47°10.0' N, 13°16.3' E), three rock fall events occurred in the year of 2019 (Figure 1) on the 25th of March, 15th of July, and 24th of October.

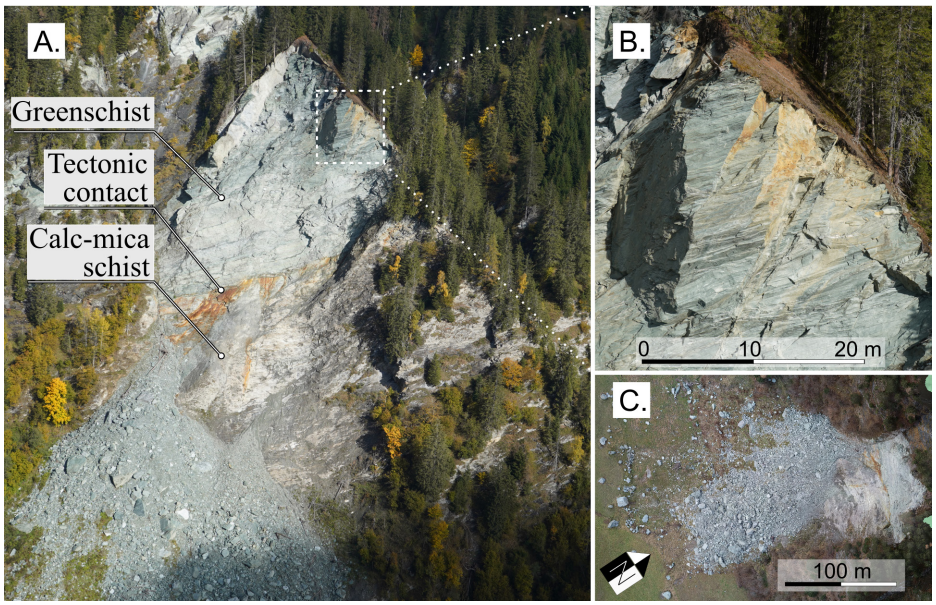

Figure 1. Situation after the third and latest rock fall event: A. Overview of the rupture surface; B. Overhanging, metastable rock mass; C. Orthophoto of the rock fall site.

The cumulative failure volume amounted to circa 30 000 m^3 and originated from a 250 m high, sub-vertical rock slope (Figure 1, A. & B.). The largest blocks showed volumes of up to 300 m^3 and hit the valley bottom (Figure 1, C.). The unstable slope from which the rock falls originated is composed of greenschist rocks in its upper and calc-mica schists in its lower section. Both lithologies are highly schistose and separated by a weathered, tectonic contact parallel to their schistosity (Figure 1, A). They are allocated to the 'Bündnerschiefer' of the eastern Tauern Window, e.g. Exner (1956), or the Glockner Nappe System, e.g. Pestal et al. (2009), in more recent classifications. The exposed rock mass at the Hüttschlag rock fall site shows several sets of tectonically inherited discontinuities described below.

3 STRUCTURAL & KINEAMTIC ANALYSIS

In the field, we recorded discontinuities in Clar-Notation (dip direction/dip angle), i.e. joints, faults, and slickensides, on the stable rock faces surrounding the rock fall. By using the cluster analysis tool of the software DIPS (Rocscience 2020), we identified three discontinuity sets (Figure 2, A.).

Set 1 is characterized by a mean orientation of 218/60 and dips steeply out of the slope, which itself has an orientation of 215/85. The sub-vertical discontinuities of Set 2 show a mean orientation of 124/78 and are orientated orthogonally to the mean of Set 1. Furthermore, Set 3 represents the schistosity and sub-parallel discontinuities, which dip obliquely into the slope with a mean orientation of 001/40.

These discontinuity sets are visible on the exposed rupture surface (Figure 2, B.). The rupture surface can further be divided into two parts: i) a lower part, characterized by a plane, polished surface, which is allocated to a pre-existing discontinuity of Set 1, and ii) an upper part showing a stepped, rougher surface. It is assumed that the rough surface in the upper part was formed by the rock fall process itself, i.e. by the coalescence of variably oriented discontinuities and brittle rock bridge failure.

Field evidence clearly suggests, that the structural inventory had a decisive impact on the rock fall process (compare Figure 2 A. to B.). Based on the structural inventory, we conducted a kinematic analysis (discontinuity poles and intersection vectors), to analyse which failure mechanisms are likely to reproduce the event.

The kinematic analysis based on the pole density (Figure 2, C.) shows that the orientation of Set 1 favours the development of a planar sliding mechanism, as it dips out of the slope at a dip angle less steep than the slope itself. Since there is no discontinuity set present, which dips steeply into the slope, a flexural toppling mechanism can be excluded.

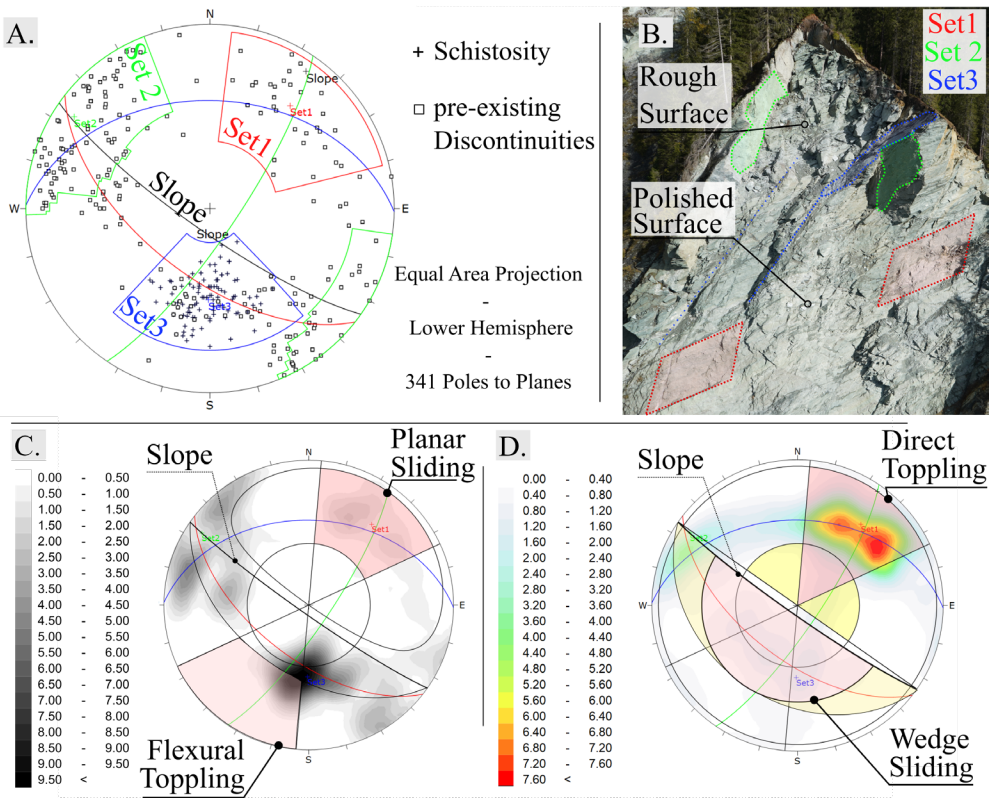

Figure 2. A. Discontinuities recorded in the field with their discontinuity sets (Set 1, 2, 3) identified by cluster analysis; B. The identified discontinuity sets projected on the rupture surface; C. Kinematic analysis for pole density concentration and; D. For intersection vector density.

When looking at the density distribution of intersection vectors (Figure 2, D.) we find that two intersections are critical. Firstly, the intersection of Set 2 with Set 3 results in moderately in-slope dipping vectors. They favour a direct block toppling mechanism in interplay with critical base planes of Set 1. Also, individual discontinuities of Set 3, which dip into the slope at a low angle, may function as a basal detachment. Secondly, rock wedge sliding is also kinematically possible due to the intersection of Set 1 with Set 2. The resulting vector dips steeply out of the slope. Thereby, Set 2

would provide the necessary lateral release, and Set 1 would function as a basal detachment in the same manner as outlined in the rock planar slide mechanism (Figure 2, C.) before.

To investigate which failure mechanism of these proposed end members – i.e. planar and wedge sliding or direct block toppling – is developed, we conducted a 2D distinct element modelling (DEM) study by applying the Universal Distinct Element Code (UDEC) (Itasca 2018). For our 2D UDEC model, we selected a slope profile orientated parallel to Set 2 (= lateral release for wedge sliding). This allowed to simulate both sliding mechanisms – i.e. planar and wedge sliding – using the same slope model.

4 DISTINCT ELEMENT MODELLING

We derived the pre-failure topography of the rock slope from the digital elevation model based on the airborne laser scanning campaign 2007 (https://www.salzburg.gv.at/sagis, latest access in December 2022). In our DEM, we considered the fractured rock mass as an assemblage of field-related discontinuities, i.e. joints, faults, and slickensides, and an intact rock matrix representing the blocks. A Mohr-Coulomb contact law was assigned to the discontinuities and a linear elastic constitutive relationship to the intact rock.

Since it is not possible to simulate growth and coalescence of real cracks in linear elastic blocks by UDEC (Itasca 2018), we tessellated them into small polygons, referred to as Voronoi elements (e.g. Spreafico et al. 2017). Mohr-Coulomb contact law was also assigned to the contacts of these Voronoi elements, however with different mechanical properties than for the discontinuities (see Table 1). This approach enabled us to simulate intact rock failure of blocks between pre-existing, non-fully persistent discontinuities in a simplified manner, allowing the development of a rupture surface with any geometrical shape. In our study, we integrated asymmetric Voronoi elements characterized by their longer axis being inclined according to the inclination of the schistosity. The rock mechanic properties used for the model are summarized in Table 1.

Table 1. Properties used for the UDEC model for intact rock, Voronoi contacts, and pre-existing joints.

For …	Property		Value	Unit	Reference or Comment
Intact Rock	Density	ρ	2700	kg/m^3	/
	Young´s Modulus	E	40	GPa	(BBT 2008) for intact rock in a green-schist, partly calcareous rock mass
	Poisson Number	ν	0.15		
Voronoi Contacts	Cohesion	c	0.90	MPa	(BBT 2008) for a greenschist, partly calcareous rock mass;
	Friction Angle	φ	44.00	°	
	Tensile Strength	t	0.10	MPa	Kept constant to avoid distortions
	Normal Stiffness	st_n	200	GPa	High, to prevent contact overlap (Itasca 2018)
	Shear Stiffness	st_s	100	GPa	
Pre-existing Joints	Cohesion	c	0.05	MPa	(BBT 2008) for discontinuities in a green-schist, partly calcareous rock mass;
	Friction Angle	φ	30.00	°	
	Tensile Strength	t	0.00	MPa	Fully persistent joints; no infilling
	Normal Stiffness	st_n	200	GPa	High, to prevent contact overlap (Itasca 2018)
	Shear Stiffness	st_s	100	GPa	

In order to build our DEM, we implemented the main structural inventory, as it was outlined in the kinematic analysis before (Figure 2), into the 2D pre-failure topography (Figure 3, A.). It comprised the schistosity, the intersection vector of Set 2 and Set 3 (Figure 2, C.) and the prominent joint of the rupture surface, which is related to Set 1 and was mapped in the lower part of the rock face (Figure 2 B). In order to investigate the controlling effect of the structural inventory on the rock fall failure mechanism, the trace length of this joint was varied. For one simulation run, the persistence was set to 50 % of the full length, approximating the in-situ conditions (Figure 2, B.). For a second run, 100% persistence was assumed.

The model output showed, that a persistence of 50% for the Set 1 joint, i.e. the approximated in-situ conditions, led to a detachment of several rock mass columns from the rock slope in a direct block toppling mechanism (Figure 3, B.). The toppling failure is characterized by minorly inclined displacement vectors pointing out of the slope, and by displacement magnitudes increasing upwards within the individual rock mass columns. To allow kinematic freedom for this toppling failure, new, brittle failure paths developed. They propagated upwards, e.g. from the upper tip of the Set 1 discontinuity, towards the surface. This exposed a new, rough surface, as also visible on the rock slope in nature (compare Figure 3, B. to Figure 2, B.).

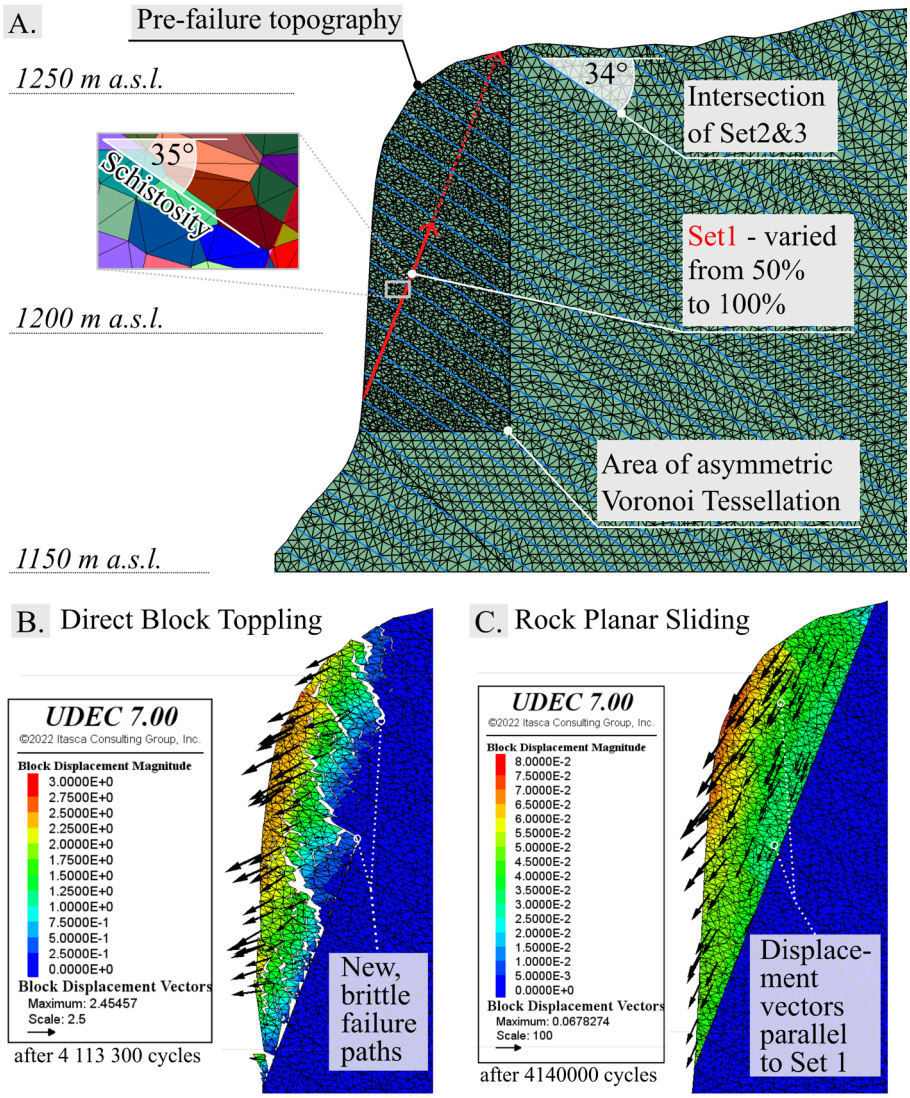

Figure 3. The DEM. A. Model input, inlet shows the inclination of the asymmetric Voronoi elements with respect to the schistosity; B. Joint of Set1 at 50% persistence and; C. At 100% persistence.

However, a remarkable observation is, that if the persistence of the Set 1 joint is increased to 100% (Figure 3, C.), the initial failure mechanism changes from direct block toppling to sliding (either planar, or wedge sliding), with the Set 1 joint as the basal sliding surface and Set 2 (i.e. the orientation of the slope profile) as lateral release. In this case, the displacement vectors are orientated sub-parallel to the surface of Set 1.

5 DISCUSSION & CONCLUSION

The failure mechanism observable in our DEM alternates between the mechanisms proposed by the kinematic analysis (compare Figure 2 C. & D. to Figure 3 B. & C.), i.e. between direct block toppling and sliding (either planar, or wedge sliding). The critical factor which governs the respective failure mechanism is the persistence of the pre-existing joint of Set 1 (compare Figure 3 B. to C.). Thus, we conclude, that for the Hüttschlag rock falls, a kinematic analysis is ambiguous and to some extent limited, since fully persistent discontinuities are assumed in such an analysis.

This imposes a challenge in rock slope engineering. Methods such as objective scanline recording, e.g. Priest (1993), and statistical analysis of the so obtained data, e.g. Zangerl et al. (2022), may be one adequate measure to address this challenge. However, non-fully persistent areas of discontinuities are generally not recognizable before failure (e.g. Shang et al. 2017) and may only be detected under certain conditions at shallow depths (Guerin et al. 2019).

Nevertheless, a kinematic analysis is a proper tool to obtain a catalogue of possible failure mechanisms (Wyllie & Mah 2004). However, its limitations become obvious in this study, in which we highlighted the ambiguity of kinematic analyses and identified discontinuity persistence as a controlling factor of rock slope failure mechanisms.

REFERENCES

BBT. 2008. *Gebirgsarten, Gebirgsverhaltenstypen, Störzone - Verbindungstunnel*. Technischer Bericht G 1.2b-05 (unpublished)

Crosta, G. B., Agliardi, F., Frattini, P., & Lari, S. 2015. Key Issues in Rock Fall Modeling, Hazard and Risk Assessment for Rockfall Protection. In: *Engineering Geology for Society and Territory*. 2, pp. 43-58

Exner, C. 1956. *Geologische Karte der Umgebung von Gastein, 1:50000*. Geologische Bundesanstalt, Wien

Goodman, R. E., & Bray, J. W. 1976. Toppling of rock slopes. In: *Proceedings of the Specialty Conference on Rock Engineering for Foundation and Slopes*. 2, pp. 201 - 234.

Guerin, A., Jaboyedoff, M., Collins, B. D., Derron, M. H., Stock, G. M., Matasci, B., Boesiger, M., Lefeuvre, C., Podladchikov, Y. Y. 2019. Detection of rock bridges by infrared thermal imaging and modelling. *Scientific reports*. 9(1), pp. 1-19. doi: 10.1038/s41598-019-49336-1

Hungr, O., Leroueil, S., & Picarelli, L. 2014. The Varnes classification of landslide types, an update. *Landslides*, 11, pp. 167 - 194. doi:10.1007/s10346-013-0436-y

Itasca. 2018. *UDEC - Universal distinct element code, Version 7.0*. User's Manual, Itasca Consulting Group, Minneapolis

Pestal, G., Hejl, E., Braunstingl, R., & Schuster, R. 2009. *Erläuterungen - Geologische Karte von Salzburg 1: 2000000*. Land Salzburg & Geologische Bundesanstalt, pp. 162

Poisel, R., & Preh, A. 2004. Rock slope initial failure mechanisms and their mechanical models. *Felsbau*, 22(2), pp. 40-45.

Priest, S. D. 1993. *Discontinuity Analysis for Rock Engineering.* Chapman & Hall, 473 p.

Rocscience. 2020. *Dips - Graphical and Statistical Analysis of Orientation Data, Version 8.003*. Software, www.rocscience.com, Toronto, Ontario, Cananda

Shang, J., Hencher, S., West, L., & Handley, K. 2017. Forensic excavation of rock masses: a technique to investigate discontinuity persistence. *Rock Mechanics and Rock Engineering*, 50, pp. 641-652. DOI: 10.1007/s00603-017-1290-3

Spreafico, M. C., Cervi, F., Francioni, M., Stead, D., & Borgatti, L. 2017. An investigation into the development of toppling at the edge of fractured rock plateaux using a numerical modelling approach. *Geomorphology*, 288, pp. 83-98.

Wyllie, D. C., & Mah, C. 2004. R*ock Slope Engineering: Civil and Mining*. 4th ed., Spon Press Taylor and Francis Group, 456 p., DOI: 10.1201/9781315274980.

Zangerl, C., Koppensteiner, M., & Strauhal, T. 2022. Semiautomated Statistical Discontinuity Analyses from Scanline Data of Fractured Rock Masses. *Applied Sciences*, 12(19), 9622, DOI: 10.3390/app12199622

Zangerl, C., Prager, C., Brandner, R., Brückl, E., Eder, S., Fellin, W., Tentschert, E., Poscher, G., & Schönlaub, H. 2008. *Methodischer Leitfaden zur prozessorientierten Bearbeitung von Massenbewegungen*. Geo. Alp, 5, pp. 1-51.